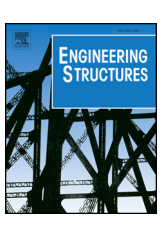
FISEVIER

Contents lists available at ScienceDirect

Engineering Structures

journal homepage: www.elsevier.com/locate/engstruct



Analysis of post-necking behavior in structural steels using a onedimensional nonlocal model



Yazhi Zhu^a, Amit Kanvinde^{b,*}, Zuanfeng Pan^a

- ^a Department of Structural Engineering, Tongji University, Shanghai 200092, China
- b Department of Civil and Environmental Engineering, University of California, Davis, CA 95616, United States

ARTICLE INFO

Keywords: Diffuse necking Strain localization Mesh sensitivity Nonlocal formulations Characteristic length Structural steels

ABSTRACT

In modeling necking in steel bars subjected to uniaxial tension using a classical one-dimensional elastoplastic continuum, numerical results exhibit strong mesh dependency without convergence upon mesh refinement. The strain localization and softening with respect to necking in structural steels is induced by hybrid material and geometric nonlinearities rather than material damage. A one-dimensional nonlocal model is proposed to address these numerical difficulties and to provide an enhanced numerical representation of necking-induced localization in structural steels for the potential implementation in fiber-based formulations. By introducing a characteristic length and a nonlocal parameter to the standard constitutive model, the enhanced nonlocal continuum provides a well-posed governing equation for the necking problem. The finite element calculations based on this one-dimensional nonlocal model give rise to objective solutions, i.e., numerical results converge under mesh refinement. In addition, the size of the necking region also exhibits mesh-independence. The characteristic length and nonlocal parameter significantly influence the post-necking response and the dimension of the necked region. Comparison of the local and global response of necking between one-dimensional analysis and 3D simulations demonstrates that the proposed model is capable of accurately characterizing the post-necking behavior. Relationships between characteristic length for the nonlocal model and the diameter of a cylindrical bar are examined. The novel contributions of the paper are: (1) providing a transparent link between the nonlocal formulation and the physics of the necking phenomenon, and (2) providing a mathematical basis for the necessity of the "over-nonlocal" formulation.

1. Introduction

Strain localization is a common phenomenon in a wide range of materials from soil and rock to concrete and metal alloys [1–4]. The key feature of this phenomenon is a rapid transition in either the displacement field or the strain field from a homogenous to a discontinuous pattern, followed by intense straining within a narrow region [5]. Another consequence of strain localization is reflected in the mechanical behavior, wherein the global stress increases with strain until localization occurs and decreases with increasing strain subsequently. The behavior after localization is commonly associated with strain softening, which results in a negative tangent modulus. Such a drop in loading carrying capacity is often regarded as a precursor to final material failure. Therefore, strain localization plays an important role in the mechanical behavior and engineering applications of many materials, including structural steels.

Strain localization is commonly observed in structural steels during

uniaxial tension testing. At a certain point in the loading history, there is a change from a uniform distribution of strain along the tensile specimen to a localized concentration of strain in a small region associated with the physical appearance of a neck. Necking instability is essentially the consequence of the competition between the deformation of the material (resulting in a reduction of cross-sectional area) and the level of the applied stress (due to hardening). At a continuum scale, structural steels generally show continuous strain hardening in which the rate of stress decreases with increasing strain. Due to this reduced rate of strain hardening, the incremental increase in the applied stress and an incremental decrease of cross-sectional area achieve balance at a point during the deformation history. This type of softening occurs even as the material continues to strain harden at every continuum location, and may be considered an "effective" softening when the stress-strain response is examined at the coupon scale (i.e., using engineering stressstrain measurements). More specifically, this softening arises because a uniaxial representation of material response fails to capture three

E-mail address: kanvinde@ucdavis.edu (A. Kanvinde).

^{*} Corresponding author.

dimensional geometric nonlinear processes that result in the loss of cross-sectional area. Beyond this balance point, an arbitrarily small imperfection may trigger localized deformation. Subsequent deformation is concentrated into the necked region until fracture ultimately occurs.

The study of strain localization in structural steels is motivated by its important effects on the strain softening behavior (which affects global component or structural response) as well as accumulated strains that are responsible for ductile fracture and damage processes [6]. In addition to its role as a precursor to fracture, necking (and more broadly, other types of localization such as local buckling) often trigger extreme limit states, such as collapse at the component or structure scale. Moreover, the state-of-the-art in structural frame simulations [7,8] typically forgo continuum finite element simulations, and rely on uniaxial representation of materials (e.g., through fiber elements [9]), even when localization-induced softening is present. These uniformly suffer from the issues of mesh-dependency, with the implication that results are dependent on numerical discretization. Thus, a rigorous analysis and mitigation of the non-objective response of localized necking-induced softening represented in a uniaxial stress-strain construct is of academic as well as professional interest. The mathematical interpretation of the non-objective outcomes is that the material stiffness matrix is no longer positive definite, and the governing equation becomes ill-posed if classical (local) uniaxial constitutive laws are used [2]. This leads to infinitely many solutions of the strain localization distribution and energy dissipation for a single case. The solution does not converge with increasing mesh refinement, resulting in the size of localization zone becoming arbitrarily small, and the load-displacement response beyond the peak point dropping very rapidly upon mesh refinement [2,10].

Maintaining a well-posed boundary value problem after the onset of necking in a tensile test for the fiber element-based model is not possible using local continuum approaches. This mesh sensitivity problem is also discussed by Mikkelsen [11]. The problems of non-objectivity and ill-posedness may be mitigated through regularization, i.e., by incorporating a length scale into the constitutive law. This length scale may be interpreted as an extrinsic parameter that reintroduces physical phenomena (three-dimensional necking), for which the uniaxial formulation cannot otherwise simulate physically. Regularization methods are generally divided into four categories: rate-dependent constitutive models [12,13], micropolar continuum models that introduce supplementary rotational degrees of freedom into the framework of the continuum mechanics [14,15], higher order strain gradient models [16], and nonlocal models [17].

Nonlocal regularization approaches are now widely used to capture strain softening as well as ductile fracture behavior in metals, and numerous nonlocal models have been proposed [17]. As discussed earlier, even though the basic mechanical behavior of ductile solids exhibits strain hardening up to ductile fracture, effective strain softening (in the uniaxial sense) may be induced by loss of cross-sectional area due to geometric nonlinearity or by the accumulation of damage (in addition to other effects such as temperature, creep). Distinct from damagetriggered strain softening, which usually occurs as a part of the constitutive response itself [18-22], necking-induced strain localization (and softening at the global/uniaxial level) occurs simultaneously with strain hardening at the continuum constitutive level. Previous developments in one-dimensional formulations for representing necking, including nonlocal [23] and strain gradient [11] approaches, as well as their finite element solutions, rely on a modification of material constitutive laws along with an associated length scale. While these approaches expediently mitigate mesh dependency, they are also phenomenological, such that the effects of necking (e.g., load-deformation response) are replicated in an observational sense without an explicit representation of the underlying physics. While this empiricism is unsatisfying in itself, it hinders generalization of the methodology (e.g., to tension components of different sizes/thicknesses - e.g., see Kolwankar

et al. [23]) and interpretation of results, especially post-localized strains in the necked region, since they are not directly associated with physical response such as the transverse geometry change. These issues are additionally problematic when the goal is to estimate point-wise continuum strains that are responsible for fracture. Motivated by this, this paper develops a one-dimensional model with a nonlocal formulation for the analysis of necking. This model provides refined understanding of the numerical problems encountered in the uniaxial simulation of necking and a methodology to mitigate these problems. From a practical standpoint, this understanding may be used to inform simulation of localization-induced softening in steel members through a uniaxial fiber construct, since current approaches for such simulation (e.g., Kolwankar et al. [23]) are based on empirical modification of effective stress-strain laws, rather than incorporation of the geometric nonlinear phenomena that result in this effective response. From a mathematical standpoint, this model is similar to previous approaches developed for damage-plasticity - e.g., see [19,20].

The paper begins by formulating the problem of necking-induced effective softening. Subsequently, a one-dimensional nonlocal formulation is presented. This is followed by spectral analysis that rigorously examines the effect of regularization on the localization problem. To demonstrate the efficacy of the proposed approach, numerical examples are presented, these confirm the mitigation of mesh-dependence. Results from the nonlocal uniaxial model are then compared to their counterparts from three-dimensional continuum finite element models of cylindrical bars, to examine the ability of the model to reproduce post-peak physical response. The paper concludes by summarizing the work and discussing its implications and limitations.

2. Problem formulation

Necking in ductile metals is a widely studied phenomenon, and has been examined under various constitutive laws, material properties, boundary conditions, geometric configurations, and numerical methods [24-26]. It has been well recognized that necking is a case of localization and instability [27] and different types of necking have been identified, namely diffuse necking, localized deformation, and propagating neck [28]. In contrast to localized necking, in which necking localizes into an infinitesimal band, diffuse necking occurs in both directions perpendicular to uniaxial loading [29]. The width of the necking region along the length of a specimen is usually on the order of the-bar radius. Fig. 1 presents an illustrative example of mechanical response and deformation pattern in a cylindrical bar subjected to uniaxial tension to demonstrate the features of diffuse necking, which is the focus of the present study. Fig. 1(a) shows the deformation patterns in the pre- and post-localization phases, whereas Fig. 1(b) shows the load-elongation curve. Fig. 1(c) shows the effective longitudinal strain distribution during the pre- and post-localization phases. Referring to Fig. 1(b), the axial force *P* increases with elongation until a peak force point is reached. Until this stage of loading history, the strain field in the entire bar is homogeneous - see Fig. 1(a) and (c). Subsequent to this, the deformation (strain) field transitions from homogeneous to non-homogenous; specifically, the localized plastic strain concentrates at diffuse necking region, and the strain decreases due to elastic unloading at the remainder of the tensile specimen to maintain equilibrium with the dropping load. The representative criterion to predict diffuse necking is due to Considère [24], which states that necking of a tensile round bar coincides with the attainment of the maximum tensile loading, and can be expressed as:

$$\frac{\partial P}{\partial \varepsilon} = 0 \tag{1}$$

where P is the uniaxial tension load (see Fig. 1(a)) and ε is the logarithmic (true) strain. Swift [30] extended Considère's criterion to biaxial stress states. In the current paper, the basis of the Considère model will be followed to analyze post-necking behavior of

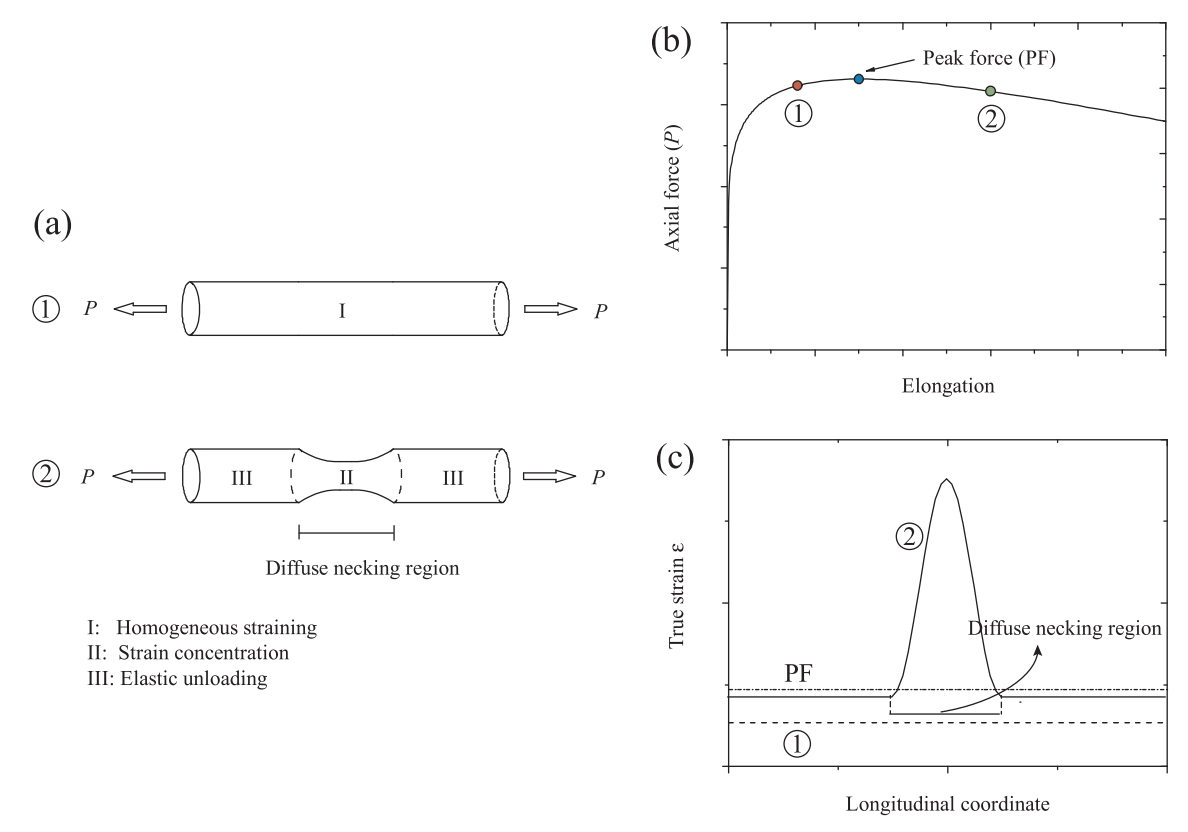


Fig. 1. Illustration of diffuse necking in a cylindrical bar: (a) deformation of the cylindrical bar; (b) load-displacement curve; (c) evolution of strain field.

homogeneous steels. The assumption of homogeneous materials excludes the possibility of microstructural heterogeneity induced necking. Let L_0 and L be the original and current length of the specimen under uniaxial tension, respectively. The incremental true strain may be expressed in terms of the change of length ΔL as:

$$\Delta \varepsilon = \frac{\Delta L}{L} \tag{2}$$

By integrating the above expression, the current deformed length may be determined from the true strain and expressed as $L=L_0e^e$, where L_0 is the undeformed length. Invoking the notion of isochoric (constant volume) plastic flow along with the approximation that volume change under elastic strains is negligible (a realistic observation for many polycrystalline metals, including structural steels) leads to the zero-volume change criterion, which may be expressed as follows:

$$A = A_0 e^{-\varepsilon} \tag{3}$$

where A and A_0 refer to the current and original area of the cross section, respectively. The relationship in Eq. (3) is exact for the regime prior to necking where the cross-sectional area remains uniform along the gauge length. In the post-necking regime, the distribution of strain is non-uniform both longitudinally and transversely. Herein, a simplification is made that the current area is related to the average longitudinal strain, which is the tensile strain at the corresponding coordinate in the one-dimensional model. This is equivalent to the assumption that the cross-sections remain planar and are perpendicular to the centerline, which is also the starting point of analysis of necking by Bridgman [25]. The uniaxial tensile load P may be expressed using the initial area of the cross section, true stress σ and true strain ε as:

$$P = A\sigma = A_0 \sigma e^{-\varepsilon} \tag{4}$$

On the other hand, material response obtained from a tensile test is often expressed in terms of the nominal (engineering) stress $s=P/A_0$. Assuming a true stress-strain response $\sigma=g(\varepsilon)$, the rate of true stress may be expressed as $\dot{\sigma}=(dg/d\varepsilon)\dot{\varepsilon}$. The rate of change of nominal stress

with respect to true strain, i.e., the tangent modulus, E_D may then be derived as:

$$\frac{ds}{d\varepsilon} = E_t = \left(\frac{dg}{d\varepsilon} - g\right)e^{-\varepsilon} \tag{5}$$

The tangent modulus is initially positive and becomes negative when $dg/d\varepsilon < g$. Herein, an exponential relationship of true stress-strain [31], which is also a common approximation for the strain hardening properties of structural steels, is employed:

$$\sigma = g(\varepsilon) = K\varepsilon^{n} \tag{6}$$

where K is the strength coefficient and n is the strain hardening exponent. To combine the two effects (i.e., strain hardening combined with geometry change) that lead to the necking type of localization, the one-dimension model represents the material coupon as a one-dimensional bar with constant area, and constitutive response representing nominal (rather than true) stress-strain behavior. Such a dimensional reduction from three dimensions to one dimension does not ensure completely consistent, physically and mathematically equivalent conversions. However, it is highly popular in engineering application since one dimensional response is recovered from standard ASTM E8 [32] coupon tests, and also used in "fiber" simulations of structural members [10]. Given the constant-area formulation, the strain hardening followed by strain softening behavior may be expressed as an effective material property:

$$\widetilde{\sigma} = g(\varepsilon)e^{-\varepsilon} \tag{7}$$

In this case, the uniaxial tensile load may be expressed as $P=A_0\widetilde{\sigma}$. In addition, to characterize the geometry effect during the deformation, a geometry parameter is introduced as:

$$k_g = 1 - e^{-\varepsilon} \tag{8}$$

The geometry parameter $k_g = 1 - A/A_0$ varies from 0 to 1, where the lower and upper bounds represent the area of the cross-section

equal to its initial value and equal to zero, respectively.

3. nonlocal approach

The nonlocal approach has been shown to effectively regularize the boundary value problem [2]. The fundamental operation of the approach is to replace the local material internal variables (e.g., equivalent plastic strain, damage variable) by their nonlocal counterparts. In contrast to the standard constitutive theories that assume that the mechanical behavior of a material point is only related to the point itself, the nonlocal approach allows the state of each material point to be related to variables in the vicinity of the material at the location of interest. From a physical standpoint, this type of nonlocality (and the associated regularization) may be interpreted as arising from processes that otherwise cannot be accommodated within classical continuum theory. For example, in the context of material damage induced softening, the nonlocality is attributed to microstructural features such as voids or secondary phase inclusions. In the context of necking, nonlocality arises due to the 3D geometric nonlinear process of neck formation that is cannot be simulated within uniaxial strain construct. From a mathematical standpoint, both strong and weak discontinuities associated with singularity and negative definiteness of the tangent stiffness matrix result in numerical instabilities that require an additional characteristic length for regularization. As mentioned above, the fundamental operation of nonlocality (in the context of the present study) is to calculate the spatial average of the quantity of interest, which may be interpreted as the localization limiter:

$$\bar{f}(x) = \frac{1}{\int_{\Omega} \alpha(x, y) dy} \int_{\Omega} \alpha(x, y) f(y) dy$$
(9)

where f is the local variable and \bar{f} is its nonlocal counterpart. The material at x is the host point that will interact with its surrounding (or receiver) points at y. The term Ω represents the volume of the structure. The term $\alpha(x,y)$ is the nonlocal weight operator, which is a function of characteristic length and the distance from the host to the receiver point. A popular form of the weight function (adopted in this study) is the Gauss error function:

$$\alpha(x, y) = \exp\left(-\pi \frac{|x - y|^2}{l^2}\right) \tag{10}$$

where l is the characteristic length. The nonlocal operator gradually diminishes from the host point to the remote point, and the weight at its center x has the greatest value $\alpha(x, x) = 1$. The normalization by the term $\int_{\Omega} \alpha(x, y) dy$ ensures that a homogenous field is not altered by the nonlocal formulation. One of the most important features of the nonlocal approach is its ability to introduce a length scale, or characteristic length – denoted as l in Eq. (10). In this study, the characteristic length is determined through 3D continuum FE simulations (with large deformations and von Mises plasticity) that directly simulate necking. More specifically, continuum FE simulations are conducted complementary to the one-dimensional nonlocal simulation, and characteristic length is then estimated by trial and error until the one-dimensional simulation can replicate both the global (load-deformation response) and the local (strain distribution) behavior in a satisfactory manner. As such, l is a considered a model parameter, which may subsequently be correlated with physical quantities (e.g., bar diameter). Using both local and global indicators in this manner results in more general and accurate calibration of the length scale [33].

3.1. Nonlocal model for post-necking analysis

The longitudinal strain is an indicator of both the strain field and the geometry change (or the geometry parameter). Consequently, it is selected as the nonlocal variable. Some facilitating assumptions are necessary to develop the nonlocal formulation. First, the change rate of longitudinal strain is decomposed into an elastic and a plastic part, i.e., $d\varepsilon = d\varepsilon_e + d\varepsilon_p$. In the context of this study (which focuses on large postnecking plastic deformations), the elastic part is negligible in comparison to the plastic strain. This leads to the following simplification:

$$\sigma = g(\varepsilon) \approx g(\varepsilon_{e0} + \varepsilon_{p}) \tag{11}$$

where ε_{e0} is the elastic strain at initial yield. Although this modification results in a minor deviation from true behavior at early stages of plasticity, the effect is modest in the post-necking phase, during which plastic strains greatly exceed the yield strain. The cross-sectional area reduction is irreversible, and arises due to the plastic deformation. For the material that undergoes elastic unloading, it is reasonable to assume that the cross-sectional geometry remains unchanged. Combining Eqs. (6), (7) and (11), the local material behavior for the one-dimensional model may be re-organized in terms of accumulated plastic strain and the yield stress:

$$\widetilde{\sigma}_{y} = \sigma_{0} \left(1 + \frac{E}{\sigma_{0}} \varepsilon_{p} \right)^{n} e^{-\varepsilon_{p}} \tag{12}$$

where $\sigma_0 = K\epsilon_{e0}^n$ is the initial yield stress. The above conversion is advantageous for two reasons. First, it facilitates the elastic predictor-plastic corrector algorithm in the numerical implementation, thereby aiding numerical convergence. Second, and perhaps more important, the total strain formulated by the nonlocal approach cannot be an effective localization limiter, since it is not guaranteed to increase monotonically while the accumulated plastic strain does. Preventing instability modes requires that the nonlocal treatment is applied to variables that increase monotonically e.g., accumulated plastic strain [2]. Following Jirásek and Rolshoven [34], a complete avoidance of mesh dependency for the localization problem induced by plastic strain softening requires a slight modification to the standard nonlocal formation. Known as the over-nonlocal formulation, this modification defines the "over-nonlocal" cumulative plastic strain using a linear combination of its local variable and nonlocal averaging counterpart:

$$\hat{\varepsilon}_p = (1 - m)\varepsilon_p + m\bar{\varepsilon}_p \tag{13}$$

where $\widehat{\varepsilon}_p$ is the over-nonlocal equivalent plastic strain, $\overline{\varepsilon}_p$ is the nonlocal average of ε_p calculated by Eq. (13), and m is the over-nonlocal parameter that is non-negative. The values of m=0 and 1 reduce the over-nonlocal model to the local plasticity model and standard nonlocal formulation, respectively. Previous research has not explicitly addressed the physical interpretations or the mathematical necessity of this parameter, other than empirically noting that a purely nonlocal model (without this adjustment) cannot completely overcome mesh dependence. To this point, the current study (in a subsequent section) provides mathematical derivations to examine this parameter, with respect to its mathematical necessity and limits.

3.2. Spectral analysis of localization

This subsection presents spectral analysis of the nonlocal formulation to examine its key features as they pertain to mathematical regularization of the problem. These include the tangent modulus of the nonlocal formulation (important from the standpoint of numerical convergence), as well as a discussion of the effects of the parameters l and m. The one-dimensional elastic constitutive equation may be expressed as:

$$\widetilde{\sigma} = E(\varepsilon - \varepsilon_p) \tag{14}$$

where $\widetilde{\sigma}$ is the current axial true stress. Based on the strain hardening/softening law in Eq. (12) and its nonlocality in Eq. (9), the local plastic variable in the plasticity model is replaced by its nonlocal counterpart, and the corresponding yield function is expressed as:

$$F(\widetilde{\sigma}, \widehat{\varepsilon}_p) = \widetilde{\sigma} - \sigma_0 \left(1 + \frac{E}{\sigma_0} \widehat{\varepsilon}_p \right)^n e^{-\widehat{\varepsilon}_p}$$
(15)

Given a plastic multiplier $\dot{\gamma}=\dot{\varepsilon}_p$, the plastic flow is required to satisfy the Kuhn-Tucker loading-unloading condition and the plastic consistency condition:

$$\dot{\gamma} \geqslant 0,$$
 $F \leqslant 0,$ $\dot{\gamma}F = 0$ and $\dot{F} = 0$ (16)

An approach proposed by Di Luzio and Bažant [35] is used to determine the exact solution of the propagation speed of stress acceleration waves. The one-dimensional bar is considered again, the length of which is assumed infinite to eliminate boundary effects. Considering the bar initially in a homogenous state of strain, i.e., $\hat{\varepsilon}(x) = \varepsilon(x) = \varepsilon_0$ and $\hat{\varepsilon}_p(x) = \varepsilon_p(x) = \varepsilon_{p0}$, the stress-strain relationship may be expressed in rate form:

$$\dot{\tilde{\sigma}} = E(\dot{\varepsilon} - \dot{\varepsilon}_p) \tag{17}$$

Accordingly, the rate form of the yield function in Eq. (17) in its initially uniform state must also satisfy:

$$\dot{F} = E(\dot{\varepsilon} - \dot{\varepsilon}_p) - \sigma_0 \left(1 + \frac{E}{\sigma_0} \hat{\varepsilon}_p \right)^{n-1} \left(\frac{nE}{\sigma_0} - 1 - \frac{E}{\sigma_0} \hat{\varepsilon}_p \right) e^{-\hat{\varepsilon}_p} \dot{\hat{\varepsilon}}_p = 0$$
(18)

Let $\hat{\sigma}_y$ be the flow stress in the yield function and the associated rate $\hat{\sigma}_y = \hat{E}_{tp} \hat{\xi}_p$, where \hat{E}_{tp} is the tangent modulus of the flow stress with respect to the plastic strain rate. Simplifying Eq. (18), the tangent modulus \hat{E}_{tp} may be derived as:

$$\widehat{E}_{tp} = \sigma_0 \left(1 + \frac{E}{\sigma_0} \widehat{\varepsilon}_p \right)^{n-1} \left(\frac{nE}{\sigma_0} - 1 - \frac{E}{\sigma_0} \widehat{\varepsilon}_p \right) e^{-\widehat{\varepsilon}_p}$$
(19)

and the uniform property leads to $\widehat{E}_{tp}(x) = E_{tp}(x) = E_{tp0}$. The harmonic wave solutions with respect to the angular frequency ω and the wave number k may be expressed as:

$$\dot{u}(x,\,t)=\dot{u}_0e^{i(kx-\omega t)}, \qquad \qquad \dot{\varepsilon}_p(x,\,t)=\dot{\varepsilon}_{p0}e^{i(kx-\omega t)}$$

(20)

Noting that $\dot{\varepsilon}(x, t) = \partial \dot{u}(x, t)/\partial x$, and recalling the equation of motion $\partial \tilde{\sigma}/\partial x = \rho \partial^2 \dot{u}/\partial t^2$, a system of linear equations is obtained by substituting the harmonic solutions into Eqs. (17) and (18):

$$\begin{cases} \{(Ek^2 - \rho\omega^2)\dot{u}_0 + Eik\dot{\varepsilon}_{p0}\}e^{i(kx - \omega t)} = 0\\ \{Eik\dot{u}_0 - \left[E + E_{tp0}\left(1 - m + \frac{m}{2l}A(k)\right)\right]\dot{\varepsilon}_{p0}\}e^{i(kx - \omega t)} = 0 \end{cases} \tag{21}$$

where $A(k) = \int_{-\infty}^{+\infty} \alpha(z) e^{ikz} dz = 2l/(1+k^2l^2)$ is the Fourier transform of the weight function in Eq. (10). To ensure non-zero solutions of \dot{u}_0 and $\dot{\varepsilon}_{p0}$, the determinant of the coefficient matrix for the linear system in Eq. (21) must equal zero, which leads to:

$$-(Ek^{2} - \rho\omega^{2})\left[E + E_{tp0}\left(1 - m + \frac{m}{2l}A(k)\right)\right] + E^{2}k^{2} = 0$$
(22)

Consequently, the angular frequency ω may be expressed as:

$$\omega = kC_e \sqrt{\frac{E_{tp0} \left(1 - m + \frac{m}{2l} A(k)\right)}{E + E_{tp0} \left(1 - m + \frac{m}{2l} A(k)\right)}}$$
(23)

where $C_e = \sqrt{E/\rho}$ is the elastic propagation velocity. The corresponding phase velocity is thus determined:

$$v_{p} = \frac{\omega}{k} = C_{e} \sqrt{\frac{E_{tp0} \left(1 - m + \frac{m}{2l} A(k)\right)}{E + E_{tp0} \left(1 - m + \frac{m}{2l} A(k)\right)}}$$
(24)

A special case of l=0 eliminates the dependency of the phase velocity on the nonlocal parameter m, which reduces the model to the local type and the phase velocity becomes imaginary. Otherwise, the

following condition needs to be maintained to ensure the velocity never becomes imaginary when the tangent modulus becomes negative:

$$1 - m + \frac{m}{2l}A(k) \le 0$$
 \Rightarrow $m \ge \frac{k^2l^2 + 1}{k^2l^2} > 1$ (25)

The basic requirement to obtain a real phase velocity is that m be greater than 1. For $m \le 1$, the term within the square root of Eq. (24) is negative, which implies the non-dispersion of the phase velocity. Next, considering the critical condition ($v_p = \omega = 0$) that leading to a static bifurcation, the corresponding critical wave number is obtained:

$$k_{cr} = \frac{1}{l} \sqrt{\frac{1}{m-1}} \tag{26}$$

The critical wavelength is:

$$\lambda_{cr} = \frac{2\pi}{k_{cr}} = 2\pi l \sqrt{m-1} \tag{27}$$

The critical value in Eq. (27) is the upper limit of wavelength, such that wave propagation is possible only below this value. The implication is that if $\lambda > \lambda_{cr}$, even a small disturbance of \dot{u} will result in an unbounded response, which is not a stable state. It is clearly seen that the critical wave length is a function of the nonlocal parameter and the characteristic length. Furthermore, $m \leq 1$ gives an imaginary value of wave length as well as the wave number; this implies that the nonlocal model regularizes the localization problem only when m > 1. The critical wavelength, which gives an approximation of the length of the localization region [35], is proportional to the length parameter for a given m.

4. Numerical implementations

Starting with the weak form of the equilibrium equation within a standard finite element framework, which is given as:

$$\int_{\Omega} \sigma \delta w d\Omega = \int_{\Omega} f w d\Omega + \int_{\Gamma} h w d\Gamma$$
(28)

where σ is the stress, w is a trial function, Γ is the boundary to the domain Ω , f is the body force, and h the force applied to the boundary Γ . The body force is neglected in this paper. Subjected to pseudo time discretization, the function in Eq. (28) may also be expressed in the incremental form as:

$$\int_{\Omega} \Delta \sigma^{n+1} \delta w d\Omega = \int_{\Gamma} f^{n+1} w d\Gamma + \int_{\Gamma} h^{n+1} w d\Gamma - \int_{\Omega} \sigma^{n} w d\Omega$$
(29)

where $\Delta \sigma^{n+1} = \sigma^{n+1} - \sigma^n$ is the stress increment at the *n*th time step. The stress increment is related to the strain increment and displacement field through the tangent modulus D^{ep} :

$$\Delta \sigma = \mathbf{D}^{ep} \Delta \varepsilon = \mathbf{D}^{ep} \frac{d\Delta \mathbf{u}}{dx} \tag{30}$$

The displacement field Δu is discretized to nodal displacements Δu_N as:

$$\Delta u = N \Delta u_N \tag{31}$$

where N is the shape function for displacement. Consequently, the strain increment may be expressed in terms of the nodal displacement field as:

$$\Delta \varepsilon = \frac{d\Delta \mathbf{u}}{dx} = \mathbf{B} \Delta \mathbf{u}_N \tag{32}$$

where $\mathbf{B} = d\mathbf{N}/dx$ is the strain-displacement matrix. Assuming the trial function \mathbf{w} is related to the nodal displacement variation, the equation in Eq. (29) is re-organized as follows:

$$\Delta \boldsymbol{u}_{N}^{n+1} \int_{\Omega} \boldsymbol{B}^{\mathsf{T}} \boldsymbol{D}_{ep}^{n+1} \boldsymbol{B} d\Omega = \int_{\Omega} \boldsymbol{f}^{n+1} \boldsymbol{N} d\Omega + \int_{\Gamma} \boldsymbol{h}^{n+1} \boldsymbol{N} d\Gamma - \int_{\Omega} \boldsymbol{B}^{\mathsf{T}} \boldsymbol{D}_{ep}^{n} \boldsymbol{B} \boldsymbol{u}_{N}^{n} d\Omega - \int_{\Omega} \boldsymbol{B}^{\mathsf{T}} \boldsymbol{\sigma}^{n} d\Omega \Rightarrow \boldsymbol{K}^{n+1} \Delta \boldsymbol{u}_{N}^{n+1} = \boldsymbol{f}_{ext}^{n+1} - \boldsymbol{f}_{int}^{n} = \Delta \boldsymbol{R}^{n+1}$$
(33)

where \pmb{K} is the global stiffness matrix, $\Delta \pmb{R}$ is the residual force vector, and $\pmb{f}_{int}^n = \int_\Omega \pmb{B}^{\rm T} \pmb{\sigma}^n d\Omega$ and $\pmb{f}_{ext}^{n+1} = \int_\Omega \pmb{f}^{n+1} N d\Omega + \int_\Gamma \pmb{h}^{n+1} N d\Gamma - \int_\Omega \pmb{B}^{\rm T} \pmb{D}_{ep}^n \pmb{B} \pmb{u}_N^n d\Omega$ are the internal and external force vector, respectively. By applying the standard Gaussian quadrature, the internal force vector may be expressed as:

$$\mathbf{f}_{int} = \sum_{i=1}^{np} w_i \mathbf{B}^T(x_i) \sigma_i \tag{34}$$

where w_i is the integration weight at Gauss point i, x_i is the coordinate of the Gauss point, and np is the total number of the Gauss integration points. The consistent tangent operator K_T is obtained by the derivative of the internal force with respect to the displacement vector, which is given as:

$$\mathbf{K}_{T} = \frac{\partial \mathbf{f}_{int}}{\partial \mathbf{u}} = \sum_{i=1}^{np} w_{i} \mathbf{B}^{T}(x_{i}) \frac{\partial \sigma_{i}}{\partial \mathbf{u}}$$
(35)

The derivative of the stress with respect to the displacement may be expressed as:

$$\frac{\partial \sigma_i}{\partial \boldsymbol{u}} = \frac{\partial \sigma_i}{\partial \varepsilon_1} \frac{\partial \varepsilon_1}{\partial \boldsymbol{u}} + \frac{\partial \sigma_i}{\partial \varepsilon_2} \frac{\partial \varepsilon_2}{\partial \boldsymbol{u}} + \dots + \frac{\partial \sigma_i}{\partial \varepsilon_{np}} \frac{\partial \varepsilon_{np}}{\partial \boldsymbol{u}}$$
(36)

In contrast to the local case, the stress at an arbitrary integration point i is the function of strains over the entire finite element mesh, which implies that the term $\partial \sigma_i/\partial \varepsilon_j$ is generally non-zero. Moreover, the derivative of strain with respect to the displacement at integration point j may be obtained as:

$$\frac{\partial \varepsilon_j}{\partial \boldsymbol{u}} = \boldsymbol{B}(x_j) \tag{37}$$

Combining Eq. (30), (35), (36) and (37) results in the consistent tangent operator as a function of the derivative $\partial \sigma_i/\partial \varepsilon_i$:

$$\mathbf{K}_{T} = \sum_{i=1}^{np} w_{i} \mathbf{B}^{T}(x_{i}) \sum_{j}^{np} D_{ij}^{ep} \mathbf{B}(x_{j})$$

$$(38)$$

where $D_{ij}^{ep}=\partial\sigma_i/\partial\varepsilon_j$ is the component of tangent stiffness matrix. Assuming the increment of the internal variable $\Delta\gamma$ equal to the incremental plastic strain ($\Delta\gamma=\Delta\varepsilon_p$), the incremental form of stress may be obtained as:

$$\Delta \sigma_i = E \left(\Delta \varepsilon_i - \Delta \gamma_i \right) \tag{39}$$

From the above equation, the incremental internal variable may be obtained as:

$$\Delta \gamma_i = \Delta \varepsilon_i - \frac{\Delta \sigma_i}{E} \tag{40}$$

Additionally, the consistent linearization of the yield function in Eq. (15) may be expressed as:

$$\Delta F_i = E(\Delta \varepsilon_i - \Delta \gamma_i) - h_i \Delta \hat{\gamma}_i = 0 \tag{41}$$

where h_i is the hardening modulus. In terms of the nonlocal internal variable, the integral form of the expression in Eq. (9) is discretized as:

$$\Delta \widehat{\gamma}_i = m \sum_{j=1}^{np} \omega_{ij} \Delta \gamma_j + (1-m) \Delta \gamma_i$$
(42)

where ω_{ij} is the integration weight of point j for the host point i, and is the function of the distance between point i and j and the characteristic length. Combining Eqs. (40), (41) and (42), the derivative $d\sigma/d\varepsilon$ is then obtained as:

$$D_{ij}^{F}$$

$$= \begin{cases} E - \frac{E^{2}}{E + (1 - m)h_{i} + m\omega_{ij}h_{i}} \\ \text{if} & i = j \\ \frac{E^{2}}{E + (1 - m)h_{j} + m\omega_{ij}h_{j}} \end{cases}$$

$$\text{if} & i \neq j$$

$$(43)$$

The tangent operator derived as above is consistent with the tangent matrix developed by Andrade et al. [36]. Compared to the local case, the tangent operator for the integral type of nonlocal formulation has more non-zero components due to the nonlocal interaction. Consequently, the bandwidth of the tangent matrix as well as the global stiffness matrix increase significantly, implying additional computational expense for the nonlocal case, as noted previously by Andrade et al. [36] and Jirásek and Patzák [37].

5. verification and validation against continuum finite element simulations

This section investigates the capability of the nonlocal formulation to mitigate mesh sensitivity and to simulate physics of diffuse necking by: (1) examining mitigation of mesh dependence of numerical FE solutions by using the proposed model, (2) examining strain and stress fields within the necked region predicted by the one-dimensional model and comparing with the full continuum finite element solutions, and (3) calibrating the characteristic length for the application of the proposed nonlocal model to the post-necking problem. Three-dimensional finite element simulations of the post-necking behavior of the cylindrical bars are used as numerical experiments to provide benchmark data for the verification of the proposed model. This is because the 3D continuum simulations directly simulate necking, and the associated effects of effective softening and localization. Moreover (unlike experiments), 3D continuum simulations provide access to the full strain field of the specimen.

As shown in Fig. 2, a one-dimensional Finite Element (FE) model is developed to represent the tension necking bar. The model consists of one-dimensional (truss) elements arranged in series. Each element uses a linear interpolation function with a single Gauss integration point at its center. To trigger the localization, an imperfection is introduced by reducing the cross-sectional area of the element at the center of the bar by 0.1%. Following Kolwankar et al. [23], the magnitude of the imperfection was selected to provide a perturbation without significantly affecting the pre-necking and post-necking response of the bar. The boundary conditions are also presented in Fig. 2, wherein one end is restrained with respect to axial displacement while the other end is subjected to the displacement Δ .

The (3D) continuum finite element model takes advantage of symmetry of the cylindrical bar, and half of a three-dimensional axisymmetric model was employed by using the solid element CAX4 (bi-linear axisymmetric element) to simulate the bar under uniaxial tension. The

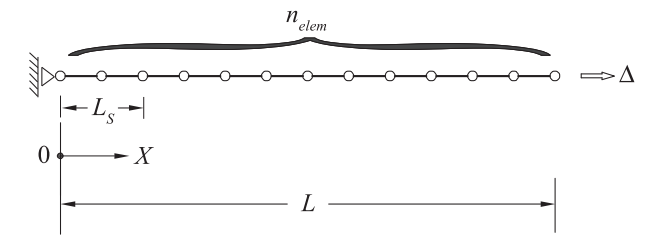


Fig. 2. Finite element representation of cylindrical bar with one-dimensional, constant area linear finite elements. (n_{elem} is the total number of the elements; L_s is the length of the localization region. Each element has an identical initial length of $L_0/2n_{elem}$.)

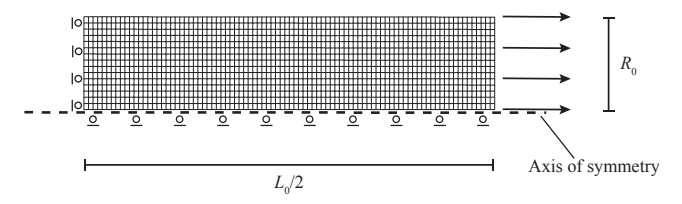


Fig. 3. Geometry and boundary conditions of the axisymmetric model for the cylindrical bars.

dimensions of the axisymmetric model are shown in Fig. 3. An imperfection is introduced to trigger necking. As shown in Fig. 3, the right-hand side end of the axisymmetric model is subjected to a uniform axial displacement and both ends are shear free. The axis of symmetry is restricted at radial deformation and is free with respect to axial displacement. The mesh was refined to obtain converged solutions for post-necking response. Note that unlike the uniaxial construct, the problem is well-posed because necking is directly simulated in 3D continuum models.

5.1. Mesh sensitivity of uniaxial models

The mesh sensitivity of the numerical solutions determined from the proposed model is examined in this subsection considering two aspects including: (1) the dependency of the numerical solutions on numerical discretization; (2) the agreement of the response predicted by the proposed model with the physical response as determined through continuum FE simulations, in terms of both the global (load-displacement) and the local (strain field) response. The comparison of the global response between the 3D and one-dimensional nonlocal analysis is straightforward. The examination of the local response focuses on geometric aspects of the necking profiles, specifically:

- For a bar with a given geometry configuration and material property, the full (3D) continuum finite element analysis is conducted to characterize pre- and post-necking response of the cylindrical bar.
 The load-displacement response as well as the strain field of the bar, particularly at post-necking stage, are used as benchmark quantities for model evaluation.
- 2. The combination of the characteristic length l and the nonlocal parameter m influences the post-necking response of the truss model; these need to be determined. According to Jirásek and Rolshoven [34] and previous spectral analysis, any selection of m > 1 is acceptable. On the other hand, this parameter significantly influences the computational cost. The reason is that a smaller nonlocal parameter m requires a larger characteristic length l to ensure that the computed size of necked region comparable to that determined through continuum FE simulations. Following the suggestion by Jirásek and Rolshoven [34], m is chosen as 4 in this paper. Based on the one-dimensional line model, the characteristic length is then calibrated by performing parametric studies to achieve a good match of the load-displacement response with the solutions obtained by the full FE analysis at pre- and post-necking stages. The number of elements (n_{elem}) of the line model is selected to ensure that the smallest characteristic length for parametric studies is larger than the initial size of each element $L_0^e = L_0/n_{elem}$.
- 3. Once the characteristic length has been calibrated as above, localized deformation fields resulting from the uniaxial nonlocal and 3D continuum models are compared. For this purpose, the quantity k_g given in Eq. (8) is particularly useful because it is an indicator of necked geometry that may be recovered from both the uniaxial and 3D models. Following the assumption that the radial strain is uniform at the necked region, the longitudinal strain in a 3D cylindrical bar may be determined as:

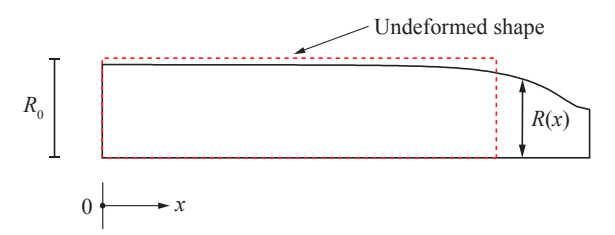


Fig. 4. Illustration of the deformed and undeformed cylindrical bar (x denotes the normalized coordinate of the cylindrical bar).

$$\varepsilon_{\text{avg}}(x) = -\ln(1 - k_g) = -2\ln\frac{R(x)}{R_0}$$
(44)

where R_0 and R(x) are the initial and current radius of the cross section, respectively (see Fig. 4). Note that the current radius R(x), the longitudinal strain calculated by both the full continuum FE model and the one-dimensional model are all the function of the longitudinal coordinate. All the three quantities are uniform in the longitudinal direction before the onset of necking and vary with the longitudinal coordinate after necking.

The above process is applied to numerical example of a cylindrical bar with the radius $R_0=0.5\,\mathrm{mm}$ and the length $L_0=20\,\mathrm{mm}$ under uniaxial tension. For the full continuum finite element model, the size of the axisymmetric elements was selected as $0.025\,\mathrm{mm}$ based on mesh sensitivity studies. For the one-dimensional model, all the elements except the one at the center (which is perturbed) of the bar have a constant unit area, i.e., $A=1\,\mathrm{mm}^2$. The material properties in terms of the initial yield stress, modulus of elasticity and hardening exponent are given as $\sigma_0=400\,\mathrm{MPa}$, $E=210\,\mathrm{GPa}$ and n=0.15 (these are realistic values for low-carbon structural steel – Kolwankar et al. [23]). Four different characteristic lengths ($l=0.05\,\mathrm{mm}$, $0.10\,\mathrm{mm}$, $0.15\,\mathrm{mm}$, $0.2\,\mathrm{mm}$) are used in the nonlocal formulation. Six different mesh refinements (101, 201, 301, 401, 501, 601 elements) are considered for the numerical discretization of the one-dimensional model.

The nominal (engineering) stress-strain response recovered from the FE simulations by using the local formulation are shown in Fig. 5(a), where the horizontal axis indicates the engineering strain Δ/L_0 calculated as the ratio of elongation to the initial length. The solid line in Fig. 5(a) refers to the response where no strain localization occurs, which means softening occurs uniformly over the entire bar beyond the instability point. After the instability point, the material undergoes effective strain softening within the localization zone with elastic unloading outside the localization region. Referring to the figure, increasing the mesh refinement leads to an earlier and sharper (i.e., steeper negative slope) drop in the stress-strain curve. The strain distributions along the length of the bar obtained by using four different discretizations are shown in Fig. 5(b). For each discretization, the strain localizes into the perturbed element of the bar model. As the mesh becomes finer, the magnitude of the localized strain increases. The length of localization zone and the internal strain are dependent on the size of the single element of the bar. As the element size becomes infinitesimal, the length of localization region also becomes infinitesimal. The numerical analysis shows difficulties in replicating the postnecking response accurately within the framework of classical continuum model. The implication is that the uniaxial material (being unable to directly simulate necking and the associated loss of area) requires an extraneous localization limiter to ensure the strain localizes into a finite and determined region at an arbitrary mesh refinement.

For the nonlocal formulation, the initial element size is chosen as 0.05 mm (equal to the smallest characteristic length) that the line model is discretized by 401 elements. The corresponding load-displacement curves computed by using various characteristic lengths as well as by the full continuum FE model is shown in Fig. 6. Referring to Fig. 6, the characteristic length $l=0.15\,\mathrm{mm}$ results in the best match of the post-necking load-displacement curve with the 3D continuum FE

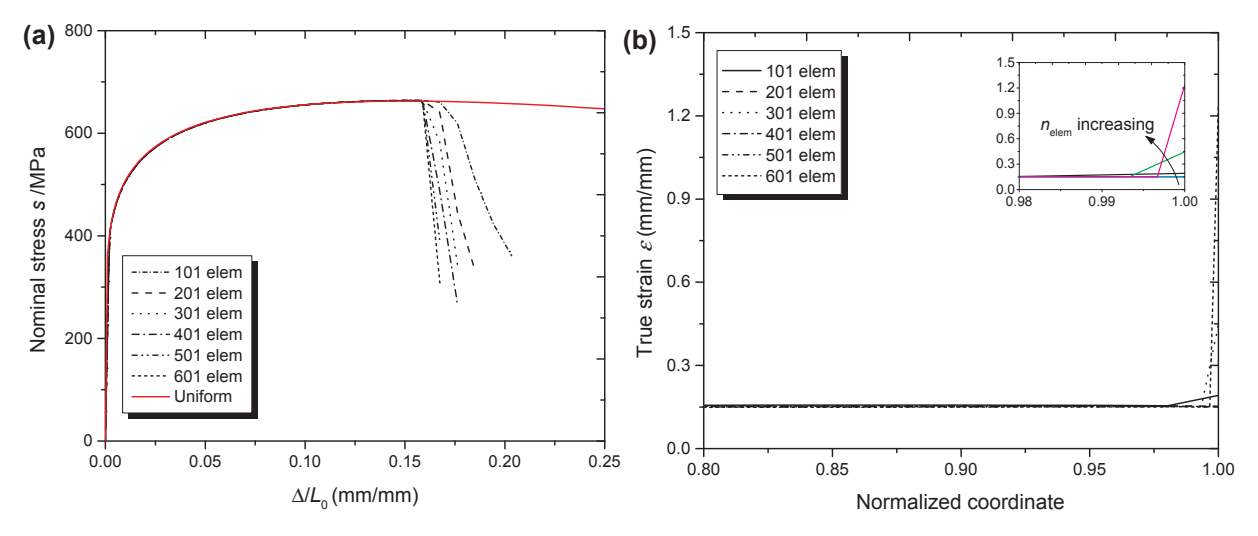


Fig. 5. The mechanical response for several mesh refinements using conventional (local) formulation (l = 0): (a) nominal stress vs. engineering strain; (b) strain distribution for several mesh refinements.

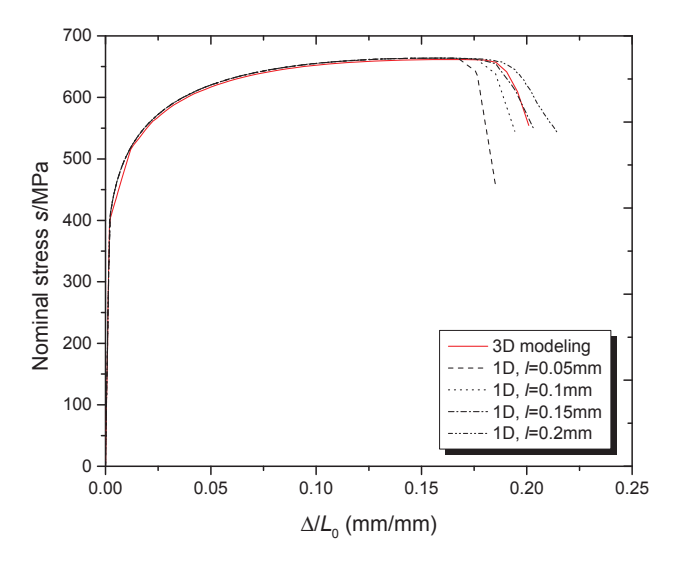


Fig. 6. Effective (engineering) stress-strain response determined from nonlocal formulation with different characteristic lengths (m = 4).

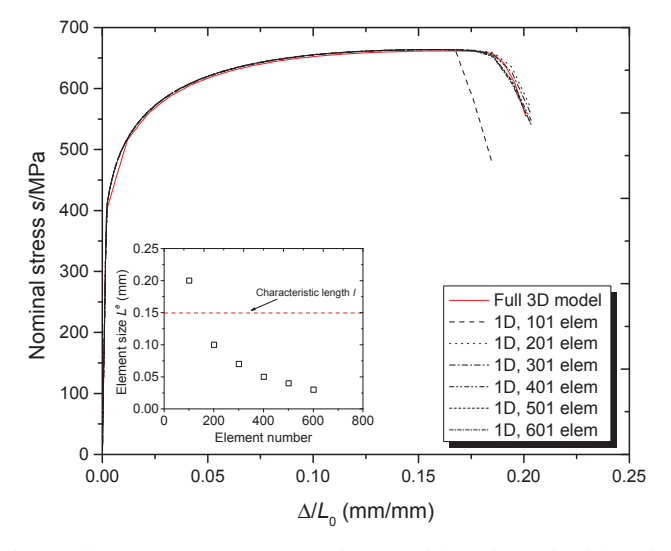


Fig. 7. Effective stress-strain response determined from the nonlocal formulation for different mesh refinements (l = 0.15 mm, m = 4).

solution. Subsequently, the calibrated characteristic length $l=0.15~\rm mm$ is used to study the mesh sensitivity with respect to the load-displacement response. The load-displacement responses calculated by using the different numerical discretizations are plotted in Fig. 7. This figure indicates that the nonlocal formulation successfully mitigates mesh-dependence, such that the various mesh refinements have similar postnecking response. An exception is noted for the coarsest mesh (101 elements) – this may be interpreted as a mesh convergence issue, in which not enough resolution is provided over the length scale to represent the variation of strain accurately. The mitigation of mesh-dependency is achieved with the element size $L^e < l$.

Fig. 8 depicts the local strain field calculated by using different mesh refinements. Fig. 8(a) compares the strain distribution along the length of the bar between 1D modeling and 3D simulation. The important observation is that as the mesh size is refined (after convergence is achieved), the localization zone does not vanish. The figure also indicates that both the length of the localization region and the shape of plastic strain profile are largely independent of the mesh. This is in sharp contrast to the results obtained by the standard constitutive law, in which the localization length is highly sensitive to mesh size (see Fig. 5(b) introduced previously). Moreover, the finite element solution exhibits behavior comparable to the continuum FE solution with respect to the length of localization region. In contrast to the sudden change in strain distribution at localization region predicted by the local formulation, a gradual (temporal) increase in plastic strain region is observed from Fig. 8(a) as loading enters the post-necking phase. Fig. 8b illustrates the peak strain at the necked region obtained by using different mesh refinements and local as well as nonlocal formulations. Referring to the results from the nonlocal formulation, the peak strain converges to the value 3D simulation when element size L^e is refined to the order of 0.05 mm ($l/L^e = 3$). For the local formulation, a decreasing size of element gives rise to an increasing peak strain (recall Fig. 5b), and no convergence is observed upon mesh refinement. The mesh independence of the strain field may be leveraged, for example in downstream damage mechanics or ductile fracture models (e.g., Besson et al. [38]).

5.2. Dependency of characteristic length on geometry

From the standpoint of application, it is useful to examine relationships between the nonlocal parameters and the geometric of the tension bar. To this end, three-dimensional models with identical lengths $L_0=20\,\mathrm{mm}$ and four different radiuses ($R_0=0.5\,\mathrm{mm}$, 0.67 mm, 1 mm, 2 mm) are studied. As discussed above, the procedure

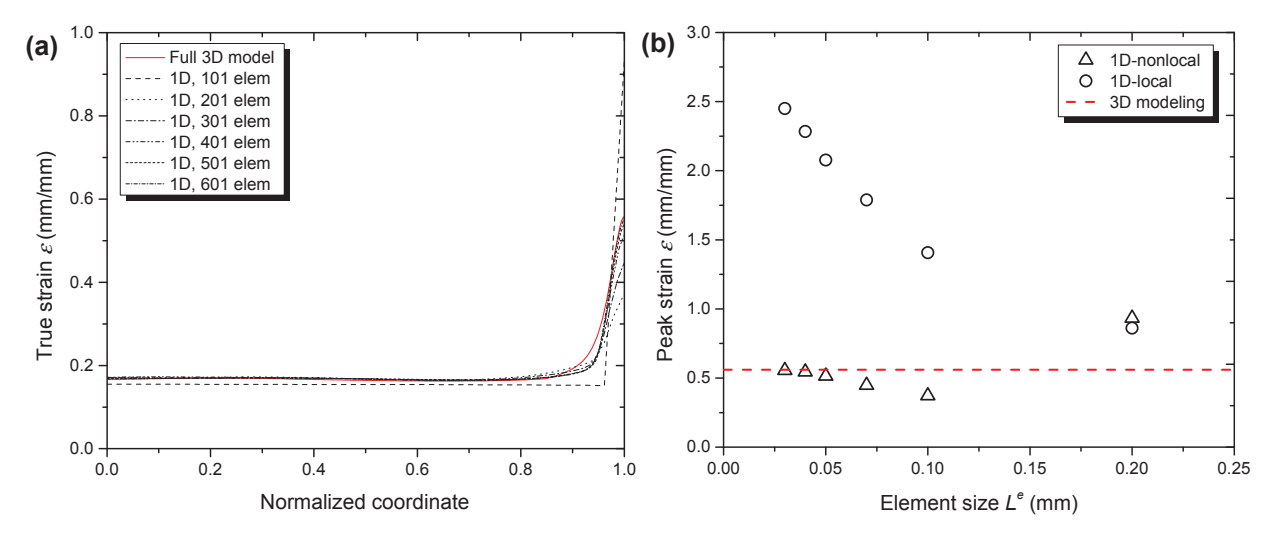


Fig. 8. Strain results for different mesh refinements: (a) strain distribution along the length of the bar; (b) peak strain for different mesh refinements by both local and nonlocal formulations.

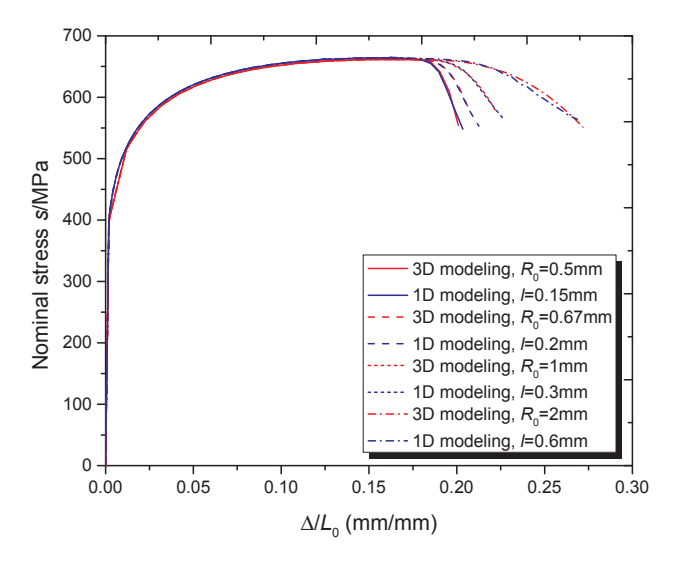


Fig. 9. Effective stress-strain curves determined through 1D (nonlocal) and 3D simulations for the cylindrical bars with different radiuses.

for the evaluation of the proposed model consists of two steps including the calibration of the model parameters and the validation. The 3D simulations again provide the basis for the evaluation. The nominal stress-strain curves for the cylindrical bars with different radiuses from 3D simulations are depicted in Fig. 9. As expected, the pre-necking response is independent on the transverse geometry (radius). At postnecking stage, the response for the cylindrical bar with a lower radius exhibits an earlier and more dramatically sudden drop in nominal stress. The results obtained from 1D analysis with various characteristic

lengths ($l = 0.15 \,\mathrm{mm}, \, 0.2 \,\mathrm{mm}, \, 0.3 \,\mathrm{mm}, \, 0.6 \,\mathrm{mm}$) were found to match the response of the cylindrical bars with four different radiuses $(R_0 = 0.5 \,\mathrm{mm}, \, 0.67 \,\mathrm{mm}, \, 1 \,\mathrm{mm}, \, 2 \,\mathrm{mm})$, respectively. Validation was also performed by comparing the longitudinal strain at post-necking stage between 1D and 3D modeling, and the results shown in Fig. 10 demonstrate good matches of 1D analyses with 3D simulations. This suggests that the length parameter is strongly related (through a linear relationship) to the initial radius of the cylindrical bar, such the length parameter may be approximately correlated with the radius as l = 0.3 R_0 . Combining Eq. (27) and the relation $l = 0.3 R_0$ and applying the value of the nonlocal parameter m = 4 gives rise to the estimated size of necked region as a function of the radius of the bar that $L_s = 3.3 R_0$. It is relevant to note that the analytical solution of the size of the necked region was derived based on the Gauss-error weight function. Other type of weight functions may result in different relationships between the length parameter and the radius. In addition, it is noted that the discussion presented in this section disregards the effect of the longitudinal geometry of the cylindrical bar (e.g., transverse edge boundary conditions). This is a fair assumption, because the bar considered in this section is of large slenderness ($L_0 / 2R_0 \ge 5$), which has applications in structural components such are reinforcement bars, tension rods, and other slender elements subject to necking.

6. conclusions

Significant attention has been drawn to the mesh dependency problem when modeling the post-necking material behavior for structural steels through one-dimensional (fiber) elements. This problem is confirmed to be inevitable within the framework of conventional approaches that use an effective softening constitutive law to simulate post-peak response. This paper examines this mesh dependence from a

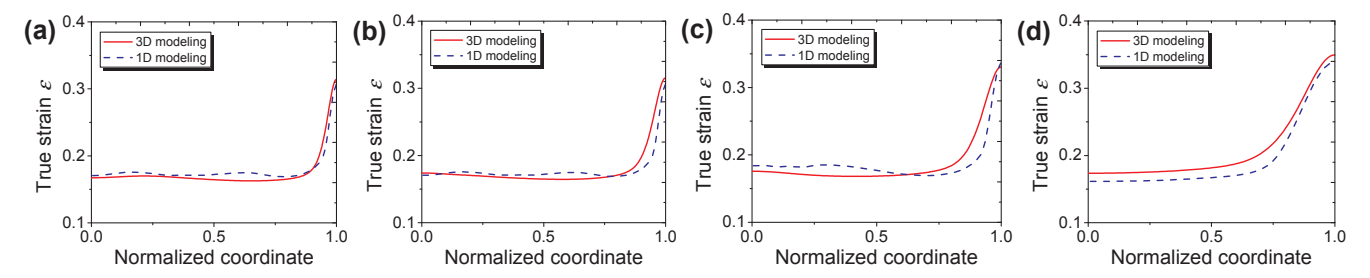


Fig. 10. Comparison of longitudinal strain between 1D and 3D modeling: (a) l = 0.15 mm, $R_0 = 0.5$ mm; (b) l = 0.2 mm, $R_0 = 0.67$ mm; (c) l = 0.3 mm, $R_0 = 1$ mm; (d) l = 0.6 mm, $R_0 = 2$ mm.

mathematical perspective, and outlines a nonlocal one-dimensional model (and its numerical implementation) to simulate post-peak response. The approach differs from prior formulations in two significant ways: (1) it explicitly represents cross-sectional geometry change in the formulation, rather than just modifying the stress-strain laws in a phenomenological manner, and (2) it provides a rigorous explanation, based on spectral analysis of localization for the empirically observed limit on the nonlocal parameter m.

Necking, which is a strain localization phenomenon in uniaxial tension specimens, is the consequence of geometric nonlinearity, in which longitudinal strain and volume conservation result in the loss of transverse area, coupling the longitudinal and transverse response. This geometry effect manifests itself as material softening, when coupon response is considered in a one-dimensional sense. This results in effective strain-softening accompanied by diffused necking. A nonlocal strain formulation is shown to regularize this problem. This approach substitutes the local plastic strain (as it is used within a softening constitutive response) by its nonlocal counterpart. This approach explicitly introduces a length scale into the problem; this length scale may be interpreted mathematically as a localization limiter, and physically, as an indicator of 3D processes that control necking, which cannot otherwise be simulated in the one-dimensional model. The main features of the model and its validation are now summarized:

- The analytical solutions for the nonlocal model are well-posed, resulting in a constant length of the localization region. An important theoretical finding is that an over-nonlocal approach is necessary from the standpoint of regularizing this problem completely. This theoretical finding validates empirical observations of previous studies.
- 2. Numerical validation studies are conducted to examine mesh-dependency of finite element solutions once the well-posedness of the problem (with the nonlocal formulation) is demonstrated. The results indicate that the size, the plastic strain distribution of the necked region as well as the load-displacement response are dependent on the nonlocal parameter and the characteristic length rather than numerical discretizations. Consequently, the identification procedure for both parameters (m, l) requires consideration of both the global material response, and also the local measurement, i.e., the details of the localization region. Subsequently, 3D simulations of post-necking behavior in a cylindrical bar are carried out to compare with the analysis by the proposed one-dimensional model. The numerical results from 1D analysis are in good agreement with those from the full 3D continuum finite element models.
- 3. The influence of the radius of cylindrical bar (i.e. slenderness) on the post-necking response is investigated. With the calibrated nonlocal parameters (m, l), the proposed model is shown to represent the global mechanical behavior and the local geometry as well as the strain field at the necked region with good accuracy for steel round bars for various values of slenderness $(L_0/2R_0 \ge 5)$. The relationship between the slenderness and the characteristic length is also estimated.
- 4. Potential applications of the proposed model include the following: (1) the concept and framework of the proposed may be conveniently generalized to regularize constitutive response for local buckling in a cross section or rebar buckling, wherein local-buckling driven strain localization is represented as a mixed material and geometry induced localization; (2) the proposed model can be incorporated into a fiber-type framework for the enhancement of beam-column elements to represent the post-necking response of a single-fiber within a cross section – similar work has been carried out by Kolwankar et al., [39].
- 5. Shortcomings of this one-dimensional model restrict its applications to the diffuse type of necking in the uniaxial tension case. Analysis of geometry induced localization in other situations (e.g., localized necking occurring inclined to the longitudinal direction) than in

diffuse necking cannot be addressed in this model. Likewise, the model (being based on an average strain at a given cross-section) does not contain information regarding the transverse strain or stress field. If such level of detail is required, then 2D or 3D continuum simulations must be conducted.

In summary, the proposed one-dimensional model provides good representation of post-necking response in structural steels, while mitigating spurious mesh dependency that is otherwise problematic when modeling post-necking behavior through conventional one-dimensional elements. While the formulation, in theory, admits prismatic members of any cross-section, it has been examined only against round bars. Further development is needed for its extension to members of arbitrary cross-section. An extension of the present model (and its attributes) to fiber-based beam- column elements is also desirable, since this has the potential of directly enhancing structural performance assessment in which necking (and more generally, localization) controls response.

Acknowledgments

The authors Yazhi Zhu and Amit Kanvinde want to thank the support of the National Science Foundation under Grant CMMI 1434300. The author Zuanfeng Pan gratefully acknowledges the funding supports of National Natural Science Foundation of China (Grant No. 51778462), and National Key Research and Development Plan, China (2017YFC1500700 and 2016YFC0701400).

Appendix A. Supplementary material

Supplementary data to this article can be found online at https://doi.org/10.1016/j.engstruct.2018.11.050.

References

- Desrues J, Bésuelle P, Lewis H. Strain localization in geomaterials. Geol Soc, London. Special Publications 2007:289(1):47–73.
- [2] Bažant ZP, Jirásek M. Nonlocal integral formulations of plasticity and damage: survey of progress. J Eng Mech 2002;128(11):1119–49.
- [3] Antolovich SD, Armstrong RW. Plastic strain localization in metals: origins and consequences. Prog Mater Sci 2014;1(59):1–60.
- [4] Zhu Y, Engelhardt MD, Kiran R. Combined effects of triaxiality, Lode parameter and shear stress on void growth and coalescence. Eng Fract Mech 2018;31(199):410–37.
- [5] Borja RI. A finite element model for strain localization analysis of strongly discontinuous fields based on standard Galerkin approximation. Comput Methods Appl Mech Eng 2000:190(11–12):1529–49.
- [6] Zhu Y, Engelhardt MD. Prediction of ductile fracture for metal alloys using a shear modified void growth model. Eng Fract Mech 2018;1(190):491–513.
- [7] Deierlein G, Reinhorn A, Willford M. NEHRP seismic design technical brief no. 4-Nonlinear structural analysis for seismic design: a guide for practicing engineers; 2010 Oct 15.
- [8] Moehle JP, Mahin S, Bozorgnia Y. Modeling and acceptance criteria for seismic design and analysis of tall buildings. PEER report 2010, 111.
- [9] Spacone E, Filippou FC, Taucer FF. Fibre beam-column model for non-linear analysis of R/C frames: Part I. Formulation. Earthquake Eng Struct Dynam 1996;25(7):711–25.
- [10] De Borst R, Sluys LJ, Muhlhaus HB, et al. Fundamental issues in finite element analyses of localization of deformation. Eng Comput 1993;10(2):99–121.
- [11] Mikkelsen LP. Post-necking behaviour modelled by a gradient dependent plasticity theory. Int J Solids Struct 1997;34(35–36):4531–46.
- [12] Needleman A. Material rate dependence and mesh sensitivity in localization problems. Comput Methods Appl Mech Eng 1988;67(1):69–85.
- [13] Nacar A, Needleman A, Ortiz M. A finite element method for analyzing localization in rate dependent solids at finite strains. Comput Methods Appl Mech Eng 1989;73(3):235–58.
- [14] Cosserat E, Cosserat F. Théorie des corps déformables; 1909.
- [15] De Borst R. Simulation of strain localization: a reappraisal of the Cosserat continuum. Eng Comput 1991;8(4):317–32.
- [16] Fleck NA, Hutchinson JW. A phenomenological theory for strain gradient effects in plasticity. J Mech Phys Solids 1993;41(12):1825–57.
- [17] Jirasek M. Nonlocal models for damage and fracture: comparison of approaches. Int J Solids Struct 1998;35(31–32):4133–45.
- [18] Zhu Y, Engelhardt MD. A nonlocal triaxiality and shear dependent continuum damage model for finite strain elastoplasticity. Eur J Mech A/Solids 2018;1(71):16–33.
- [19] Belnoue JP, Nguyen GD, Korsunsky AM. A one-dimensional nonlocal damage-

- plasticity model for ductile materials. Int J Fract 2007;144(1):53-60.
- [20] Nguyen GD, Korsunsky AM, Belnoue JPH. A nonlocal coupled damage-plasticity model for the analysis of ductile failure. Int J Plast 2015;64:56–75.
- [21] Needleman A, Tvergaard V. An analysis of ductile rupture modes at a crack tip. J Mech Phys Solids 1987;35(2):151–83.
- [22] Wu S, Wang X. Mesh dependence and nonlocal regularization of one-dimensional strain softening plasticity. J Eng Mech 2010;136(11):1354–65.
- [23] Kolwankar S, Kanvinde A, Kenawy M, Kunnath S. Uniaxial nonlocal formulation for geometric nonlinearity-induced necking and buckling localization in a steel bar. J Struct Eng 2017;143(9):04017091.
- [24] Considère M. Memoire sur l'emploi du fer et de l'acier dans les constructions. Dunod; 1885.
- [25] Bridgman PW. Studies in large plastic flow and fracture. New York: McGraw-Hill; 1952.
- [26] Audoly B, Hutchinson JW. Analysis of necking based on a one-dimensional model. J Mech Phys Solids 2016;1(97):68–91.
- [27] Abed-Meraim F, Balan T, Altmeyer G. Investigation and comparative analysis of plastic instability criteria: application to forming limit diagrams. Int J Adv Manuf Technol 2014;71(5–8):1247–62.
- [28] Mohan N, Cheng J, Greer JR, Needleman A. Uniaxial tension of a class of compressible solids with plastic non-normality. J Appl Mech 2013;80(4):040912.
- [29] Hosford WF, Caddell RM. Metal forming: mechanics and metallurgy. Cambridge University Press; 2011.

- [30] Swift H. Plastic instability under plane stress. J Mech Phys Solids 1952;1(1):1-8.
- [31] Ramberg W, Osgood WR. Description of stress-strain curves by three parameters. Tech. Note 902. Nation Advisory Committee Aeronaut 1943.
- [32] ASTM American Society for Testing and Materials. Standard test methods for tension testing of metallic materials. ASTM Int 2009.
- [33] Geers MG, De Borst R, Peijs T. Mixed numerical-experimental identification of non-local characteristics of random-fibre-reinforced composites. Compos Sci Technol 1999;59(10):1569–78.
- [34] Jirásek M, Rolshoven S. Comparison of integral-type nonlocal plasticity models for strain-softening materials. Int J Eng Sci 2003;41(13–14):1553–602.
- [35] Di Luzio G, Bažant ZP. Spectral analysis of localization in nonlocal and over-non-local materials with softening plasticity or damage. Int J Solids Struct 2005;42(23):6071–100.
- [36] Andrade FX, Pires FA, De Sa JC. Consistent tangent operators for implicit non-local models of integral type. Comput Struct 2014;1(141):59–73.
- [37] Jirásek M, Patzák B. Consistent tangent stiffness for nonlocal damage models. Comput Struct 2002;80(14–15):1279–93.
- [38] Besson J, Moinereau D, Steglich D, editors. Local approach to fracture. Presses des MINES: 2006.
- [39] Kolwankar S, Kanvinde A, Kenawy M, Lignos D, Kunnath S. Simulating local buckling-induced softening in steel members using an equivalent nonlocal material model in displacement-based fiber elements. J Struct Eng 2018;144(10):04018192.